12-3-2013

Mechanical Properties of Hydrated Acoustically Sensitive Alginate-Based Microcapsules Confined in a Microfluidic Device as a Function of Size and Composition

Maryam Mobed-Miremadi
Santa Clara University, mmobedmiremadi@scu.edu

Mallika Keralapura

Tiffany Fong

Rogel Camba

Recommended Citation

Mobed-Miremadi M, Keralapura M, Fong T, Camba R (2013) Mechanical Properties of Hydrated Acoustically Sensitive Alginate-Based Microcapsules Confined in a Microfluidic Device as a Function of Size and Composition. J Biotechnol Biomater 3:161. doi:10.4172/2155-952X.1000161

Journal of Biotechnology & Biomaterials

Mobed-Miremadi et al., J Biotechnol Biomater 2013, 3:4
DOI: 10.4172/2155-952X.1000161

Research Article Open Access

Mechanical Properties of Hydrated Acoustically Sensitive Alginate-Based Microcapsules Confined in a Microfluidic Device as a Function of Size and Composition

Dr. Maryam Mobed-Miremadi[1]*, Dr. Mallika Keralapura[2], Tiffany Fong[3] and RogelCamba[4]

[1]*Department of Bioengineering, Santa Clara University, Santa Clara, CA, USA*

[2]*U-systems, A GE Healthcare Company, Sunnyvale, CA, USA*

[3]*Biomedical, Chemical and Materials Engineering, San Jose State University, CA, USA*

[4]*Biomedical, Chemical and Materials Engineering, San Jose State University, CA, USA*

Abstract

Understanding the mechanical properties of alginate-based microcapsules according to size and chemical composition allows researchers to zero in on the treatment and methods required to engineer optimized implantable alginate-based artificial cells for chemotherapy. Cross-linked medium viscosity alginate capsules ranging from 1.1% (w/v)-1.8% (w/v) in composition and 200 μm-1200 μm in size, encapsulating ultrasound contrast agents and blue dextran were compressed within a 40 μm high polydimethylsiloxane microfluidic device and subsequently examined using 2D microscopy for strain deformation aimed at the calculation of poisson ratios and volume loss post-compression. Results indicate a decrease in Poisson ratio as a function of alginate concentration, with statistically significant increases in Poisson ratios and percent volume loss as a function of size and composition. For an average of 120 s observation time post compression, in light of the volume loss correlated to the number of cross-links as a function of capsule size and alginate concentration, a strong case for the dominance of poroelasticity vs. viscoelasticity can be made. While there was a decrease in mean Poisson ratio as a function of concentration, at 1.8% (w/v) the mean strain value converged to 0.5, the theoretical ideal isotropic value associated with soft biological tissue.

Keywords: Alginate; Acoustically sensitive microcapsules; Microfluidic device; Poisson ratio; Concentration polarization

Introduction

For the past 30 years, biocompatible hydrogels namely agarose, alginate, chitosan, collagen, fibrin and hyaluronic acid have been extensively used in drug delivery, tissue engineering and regenerative medicine due to their biocompatibility, viscoelastic characteristics, and ease of fabrication into specific shapes and sizes namely microcapsules, microfibers and patches [1-4]. Amongst, the emerging applications are engineering of micro-environments for eukaryotic cell differentiation [5-7] and implantation for ultrasound-mediated localized drug delivery [8,9]. In tissue engineering the challenge is to replicate the native tissues' mechanical and viscoelastic properties [10]. In drug delivery, the challenge is the simultaneous optimization of mechanical strength dictated by implantation site and rate of diffusion governed in turn by size and membrane permeability [11].

Biocompatible hydrogels can be modeled as viscoelastic materials that exhibit rubber like characteristics [12-15]. Because of their highly water-swollen nature, hydrogels might lose water if they are deformed, causing changes in the mechanical properties of the gel. The deformation of these elastomeric gels is time-dependent, resulting from concurrent molecular processes. The stress–strain relationship obtained from conventional testing therefore reflects a combination of the intrinsic mechanical properties of the matrix itself and its permeability [16,17]. For a given gel, measured properties will depend on liquid flows, and therefore upon the size of the particle as well as the time scale of the observations [18,19]. Concurrent time-dependent viscoelasticity and poroelasticity have been observed in many materials. In living tissues and cells, viscoelasticity results from the conformational change of macromolecules and poroelasticity results from the migration small molecules [20,21] Values of the viscoelastic relaxation time τ_v and the material-specific length $(D\tau_v)^{1/2}$ where D is the solvent diffusivity vary greatly among different materials. For a given polymer-solvent pair, the values of τ_v and $(D\tau_v)^{1/2}$ also depend on the crosslink density of the polymer network, the concentration of the solvent; multiple times are also possible for different molecular processes of relaxation [14].

Several systems have been reported in the literature for testing mechanical properties of hydrogels like microcapsules ranging from a hundreds of μm to mm range or porous slabs [19,22-33]. Some setups use indenters [19,22-27] and others use parallel plates [16,22,25,27] to compress a single microcapsule or multiple microcapsules [28]. More recent work involves the use of a MEMS force sensor [33] or texture analyzers [29-31]. In general, all mechanical testing was done on single microcapsules with the size ranging from a few microns to the millimeter scale. Various types of capsules were tested – most common being alginate, alginate chitosan, chitosan-genipin and melamine formaldehyde filled with a liquid. Effects of the encapsulated liquid on mechanical strength were not addressed. Membrane thickness was also a parameter that was studied [28,31]. It was found that a capsule with increased membrane thickness was able to sustain more force before busting. In terms of the mechanical properties measured,

***Corresponding author:** Dr. Maryam Mobed-Miremadi, Department of Bioengineering, Santa Clara University, Santa Clara, CA 95053-0583, USA, Tel: 408-554-2731; E-mail: mmobedmiremadi@scu.edu

Received October 18, 2013; **Accepted** November 27, 2013; **Published** December 03, 2013

Citation: Mobed-Miremadi M, Keralapura M, Fong T, Camba R (2013) Mechanical Properties of Hydrated Acoustically Sensitive Alginate-Based Microcapsules Confined in a Microfluidic Device as a Function of Size and Composition. J Biotechnol Biomater 3: 161. doi:10.4172/2155-952X.1000161

bursting force [19,24,26,29,31,32] and/or pressure [23,24,32] was most commonly measured. Also Young's modulus [17, 23,28,30,33], rupture strength [29], deformability [20,29,31,32] and percentage strain at burst [31,32] were other properties measured by these systems. Additional research has been conducted on cross-linked alginates and cell clusters in terms of length observation time (t) and contact length (L) in order to differentiate viscoelasticity from poroelasticity in terms of (τ_v). The time-dependent processes should occur under either the condition $t \sim \tau_v$ for viscoelastic relaxation or the condition $t \sim L^2/D$ for poroelastic relaxation [34-41].

The specific aim of this research is to map compression effects on Acoustically Sensitive Microcapsules (ASMs) of different size and membrane composition in an aqueous environment using a custom-designed microfluidic set-up. Results obtained from the stress test recorded using 2D microscopy, will be used for a twofold characterization subjected to statistical analysis. Variations in capsule strain expressed in terms of Poisson ratio, and, volume compression expressed in terms of percentage volume loss will serve as indicators of viscoelastic and poroelastic deformation, respectively. Based on the findings an ideal set of size and alginate composition be identified for future ultra-sound based drug release. Shown in Figure 1a is a micrograph of ASMs encapsulating blue dextran as a MW marker and Ultrasound Contrast Agents (UCAs). Shown in Figure 1b is a localized ASM membrane burst post ultrasound treatment.

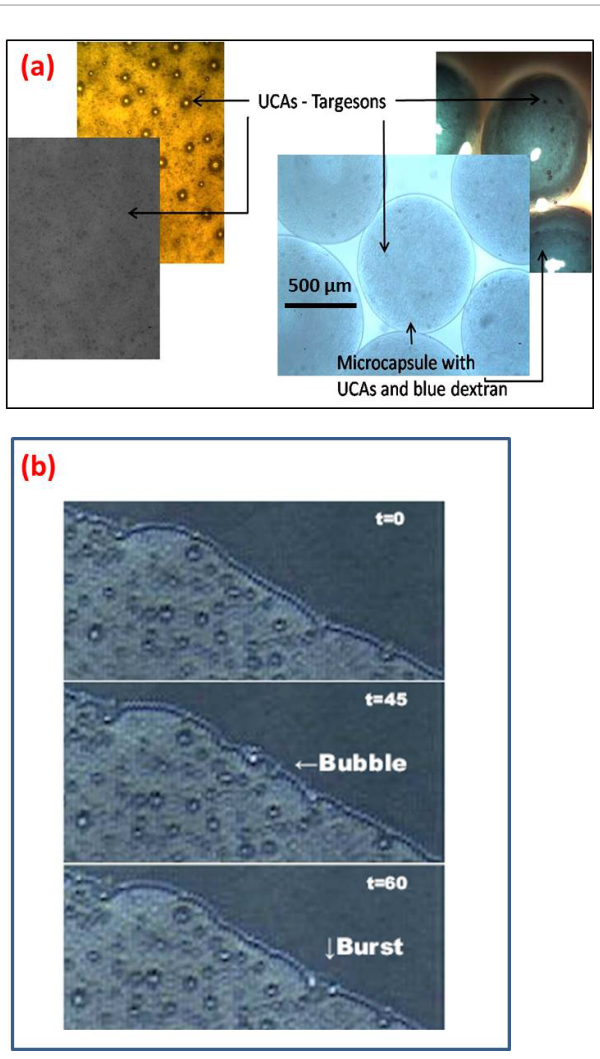

Figure 1: Micrographs of ASMs; (a): ASMs encapsulating blue dextran and ultrasound contrast agents, and (b) Chronological capsule membrane changes under ultrasound.

Materials and Methods

Polydimethylsiloxane microfluidics device fabrication

Polydimethylsiloxane (PDMS) microfluidics devices were created using the procedures for rapid prototyping of PDMS microfluidic systems [9,42]. These steps included: (1) spin-coating a single layer of SU-8 (SU-8 2035, Micro-Chem Corp., Newton, MA) onto a silicon wafer, (2) creating a photo-pattern via UV radiation exposure, (3) developing photoresist and leaving a master, (4) vapor-treating the surface with tridecafluorooctyltrichlorosilane and vacuum-casting the PDMS solution, (5) curing the PDMS layer at 150°C and then releasing it from the SU-8 master, and (6) plasma-treating and bonding the PDMS microfluidics device to a glass slide.

A 500 µm thick PDMS microfluidics device was made. The procedure included mixing 5 g of elastomer base to 1 g of curing agent (Sylgard 184 Silicone elastomer kit, Dow Corning Corp., Midland, Michigan, USA). The solution was stirred thoroughly for two minutes and placed into a vacuum chamber. The vacuum chamber was sealed and the vacuum turned on. Using a switch valve between the vacuum pump and vacuum chamber, air was quickly released every one to two minutes. Cycling between vacuum pressure and atmospheric pressure during the degassing process aided in the removal of air bubbles that formed in the solution during the elastomer base and curing agent mixing process. Once the air bubbles were removed, the vacuum was turned off and the degassed solution was removed from the vacuum chamber and poured onto the SU-8 master.

Microcapsule fabrication

Microcapsules were fabricated using the mechanism of ionotropic gelation of medium viscosity alginate (A2033, Sigma Aldrich, St. Louis, MO, USA) by means of atomization [43]. The following 3 alginate concentrations 1.1 % (w/v) (**G1**), 1.5% (w/v) (**G2**) and 1.8% (w/v) (**G3**) were used in this study where a sodium-alginate solution was jetted into a 1.5% $CaCl_2$ bath. This concentration range was chosen to encompass the wider 2%- 3% (w/v) for reported pre-sterilized alginate concentration range used in cell microencapsulation [1]. The cross-linking time was set to 1hr. The air (F_A) and liquid (F_L) flow rates were adjusted to accommodate the hydrogel viscosity and surface tension for producing a target range of 200 µm-1500 µm microcapsules at each alginate concentration. The atomizer needle assembly was a concentric 24 G needle surrounded by a 16 G needle, through which the sodium alginate and air flow. The calcified sodium-alginate beads were then washed with 0.9% (w/v) NaCl twice. For each run in ASM production, 5 mL of solution was required; comprising of 2.75 mL of alginate solution and 2.25 mL of blue dextran solution to which 0.3 mL of UCAs (Targesar P, Targeson, San Diego, USA) was added. The ASMs were kept in solution and stored in a 2-8°C refrigerator for a maximum of 24 hours prior to use.

Stress test and image capture

A single microcapsule was isolated at a time and examined under the microscope according to the scheme outlined in Figures 2a-2c. A small amount of saline was placed in the microfluidics device with

the microcapsule via a pipette. The solution reduced microcapsule shrinkage and maintained the equilibrium swollen state. To apply compression onto the constrained microcapsule, a 1mm thick glass slide was gently placed on top of the microfluidics device. Doing so trapped the microcapsule within microfluidics device, flattening the microcapsule into a cylindrical disk of a height equal to the depth of the microfluidics device (40 μm). The assembly was then placed on 2D light microscope stage. Capsule diameter prior and post compression in the X and Y directions was measured using a Nikon transmission microscope/camera (Nikon Eclipse *Ti-S*) equipped with an Andor Technology Interline CCD camera. The microcapsules were examined using 40X magnification using the image analysis software (NIS-Elements v.3.2.2). Diameters were measured at five random locations around the perimeter of the capsules and the average findings were recorded. It was assumed that the microcapsule height post-compression was equal to the height of the microfluidic device. The average time between the post-compression and size recording steps was 120 s.

Image Analysis

Based on the diameter lengths, the strain in both X and Y axes of the ASM were calculated using Equation 1

$$\varepsilon_{x/y} = \frac{D_{final} - D_{initial}}{D_{initial}} \quad (1)$$

Where ε is strain, $D_{initial}$ is the initial ASM diameter before compression, and D_{final} is the final microcapsule diameter after compression.

The strain in the z direction (ε_z) was calculated by using the averaged non-compressed diameter value in the X and Y directions as initial diameter and the height of the microfluidic device as the final diameter.

An average Poisson ratio (ν_{mean}) was calculated by averaging the diameters in the X and Y directions using Equation 2.

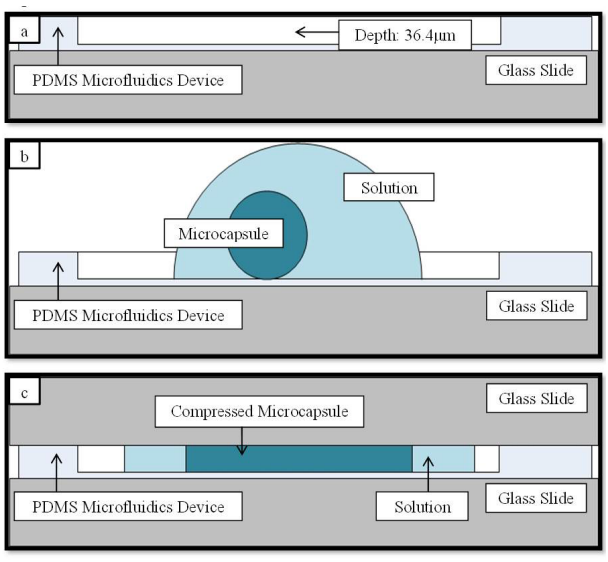

Figure 2: A side view of the PDMS microfluidics device stress test including (not drawn to scale); (a) the device before microcapsule isolation, (b) the device with the isolated microcapsule before compression and (c) the device with the isolated microcapsule after compression.

$$\nu_{mean} = -\frac{\varepsilon_{mean}}{\varepsilon_z} \quad (2)$$

The percent change in volume (%V) was also estimated by assuming a spherical shape of the microcapsules before deformation ($V_{initial}$) and a cylindrical ASM shape after compression (V_{final}). An average initial and compressed diameter was calculated by averaging the diameters in the X and Y directions. For the compressed volume, the area calculated based on the averaged volume was multiplied by the height of the microfluidic device.

Statistical Analysis

For each alginate concentration (***G1-G3***) capsules were divided according to their size into two categories, the 200 μm-500 μm (***S***) and the 500 μm above size range (***B***) in order to secure a minimum sample size 10 in each sub-population. Normality testing was conducted for the six sub-populations on Poisson ratios and percent volume compression prior to conducting a 1-sided student t-test at the 90% CI. Statistical analysis was conducted using MATLAB 2013.

Results

Filtering capsules for sphericity

Capsules were filtered for sphericity in order to deconvolute the effect of initial shape from compression. The inclusion criterion for the ratio of the axes (X/Y) was set between 0.8 and 1.25. The limits of this criterion were established based on results of screening trials where strain outlier values and capsule burst were associated with oblique capsules. Up to 20% burst was observed in the absence of filtering. Shown in Figure 3 are the pooled results of strain in the Y direction (ε_y) by size as a function of alginate concentration. As indicated by the coefficients of determination (R^2=0) approaching zero, the artifacts of morphology can be decoupled from compression effects.

Effect of capsule size on the average Poisson ratio and Volume compression

Shown in Figure 4 is a sample probability plot of the average Poisson ratio (υ_{mean}) for the population subgroup ***G1S.*** As indicated by the plot linearity, the capsules have been sampled from a normally distributed sub-population hence parametric analysis was applied to the data without any mathematical transformation [45]. All other sub-populations (***G1B***, ***G2S***, ***G2B***, ***G3S***, ***G3B***) were also subjected to Normality testing with positive results, validating the use of parametric analysis.

Results of the t-test are summarized in Table 1 as well the number of capsules analyzed per subpopulation. As indicated by the p-values (≤ 0.1), the average value of both metrics, was significantly higher for the 500 μm and higher category, hence the Null-hypothesis was accepted. The Null hypotheses were in this case that the Poisson ratio and percent volume compression were higher for the larger capsules than the smaller ones.

Although a larger surface area was constrained in contact with the microfluidic device for the ***B*** capsules than for the ***S*** subpopulation, the apex of the contact area being 40 μm the height of the channel, the capsules became stiffer with size. This finding is contradicted by tensile deformation measurements conducted on alginate ranging from 1%-3% (w/v) in concentration and several hundred micron capsules using micro-indentation [9]. With respect to volume loss due to compression leading to a net efflux of solvent, the number of cross-links in the semi-

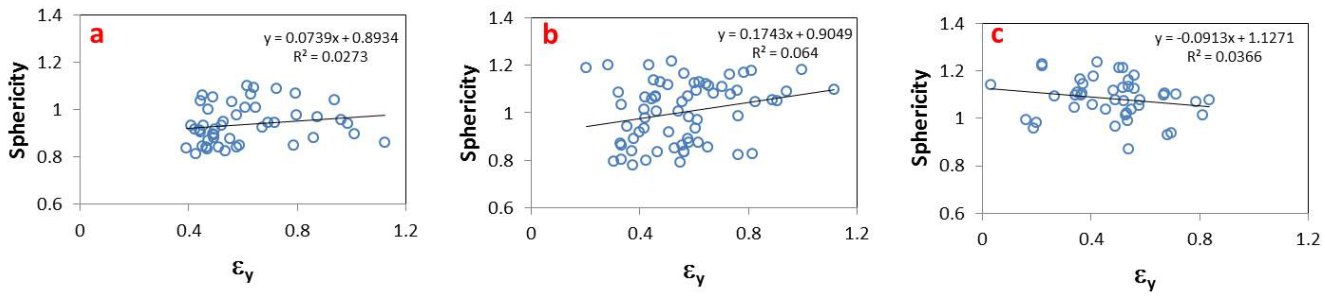

Figure 3: Capsule sphericity .vs. strain as function of alginate concentration; (a) 1.1% (w/v), (b) 1.5% (w/v), (c) 1.8% (w/v).

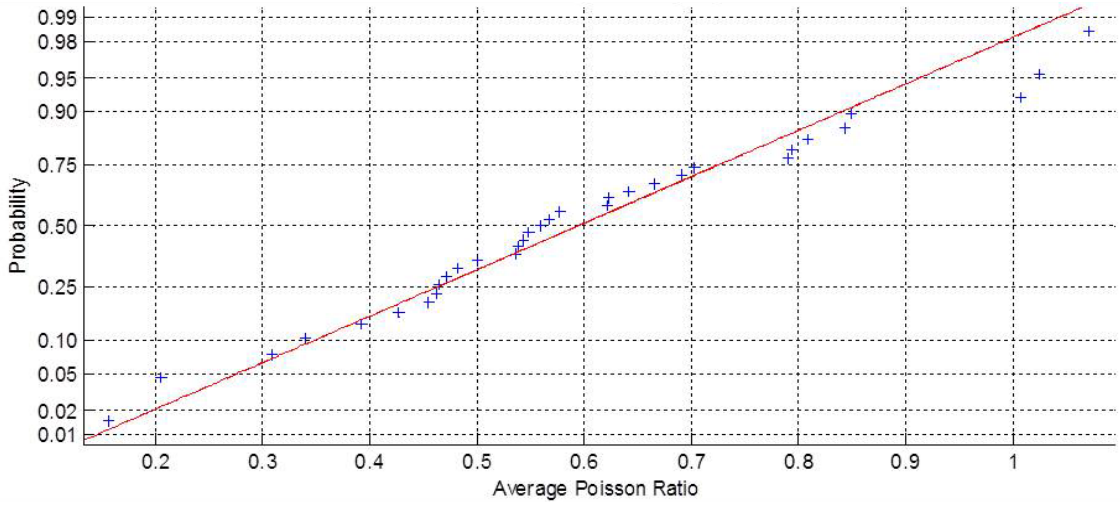

Figure 4: Half-normal probability plot for the ≤ 500 μm capsules comprised of 1.1% alginate (Subpopulation G1S).

Sample	*G1S*	*G1B*	*G2S*	*G2B*	*G3S*	*G3B*
Mean(u_{mean})	0.60	0.69	0.55	0.61	0.44	0.54
Variance(u_{mean})	0.05	0.07	0.03	0.04	0.03	0.02
N	32	26	22	42	10	32
P(T<=t)one-tail	0.097		0.101		0.041	
Sample	***G1S***	***G1B***	***G2S***	***G2B***	***G3S***	***G3B***
Mean (%V)	51.5	75.3	70.9	79.8	72.2	84.2
Variance (%V)	218.8	36.6	103.5	54.7	30.2	18.0
N	32	26	22	42	10	32
P(T<=t) one-tail	1.33E-10		8.31E-05		3.45E-09	

Table 1: Significance testing for the Poisson ratio and Percentage of Volume Compression at the 90% CI.

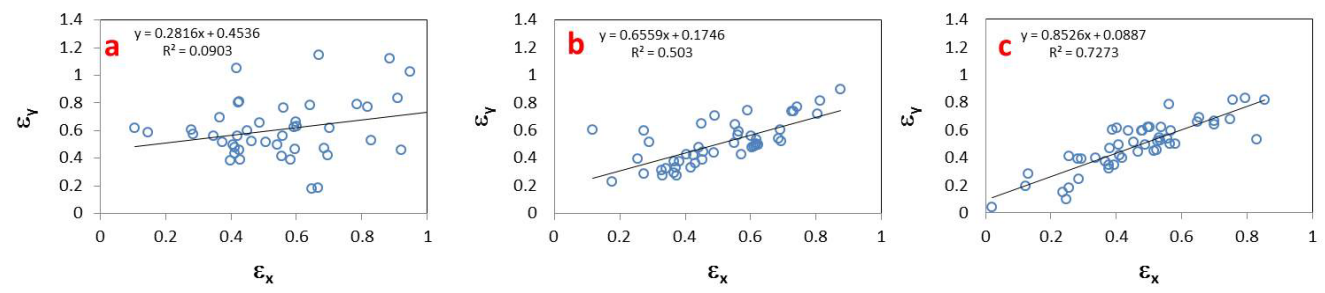

Figure 5: Correlation plots between the strain in the Y and X directions as a function of alginate concentration; (a) 1.1% (w/v), (b) 1.5% (w/v) and (c) 1.8% (w/v).

porous capsules fabricated by ionotropic gelation is proportional to the volume of the spherical structure.

Effect of alginate concentration on the Poisson ratios and Volume Compression

The correlations plots for the strain in the Y and X directions as a function of alginate content are presented in Figures 5a-5c. As shown by the progression of the coefficient of determination values (0.093, 0.503, 0.727) and slopes (0.282, 0.656, 0.853), the association between the magnitude of strain deformation in each direction became stronger with increasing alginate concentrations, inferring transition towards isotropic behavior.

Shown in Figure 6 was the monotonous decrease of the average Poisson ratio (v_{mean}) as a function of alginate concentration. At 1.8% (w/v) the mean metric value converged to 0.5 the theoretical ideal isotropic value associated with soft biological tissue [44]. Across literature an increase in the modulus of elasticity and/or an increase in strain as a function of alginate concentration are reported across multiple strain measurement techniques characterized by a wide range of measurement noise [9,28,46-48].Theoretically a decrease in the average Poisson ratio should be correlated to a decrease in strain [44]. Discrepancies between the current findings and cited literature are two-fold: 1) In the absence of measurements in the Z direction it has been assumed that the default height of the capsule post-compression is constant at 40 μm and thus an inherent error in the strain calculation was introduced, 2) Although a monotonous decrease was observed in Figure 6, experimental noise was predominant as reflected in the overlapping standard deviations. Estimating neither the modulus nor the elasticity limit was conducted in this work. It required estimating the stress on each capsule by the microfluidic device, subjecting capsules of identical size and composition to compression using multiple channel depths which is not trivial and requires separate simulations and measurements.

As for the percent volume compression, as shown in the Box plot in Figure 7 the distribution range decreased as the alginate concentration was increased and no outliers were observed at the highest concentration. A p-value of $1.4*10^{-15}$ at the 95% CI is obtained for the ANOVA conducted on microcapsules comprised of the 3 concentration groups. This analysis coupled with the examination of Figure 6 indicated an increase in volume loss as a function of alginate

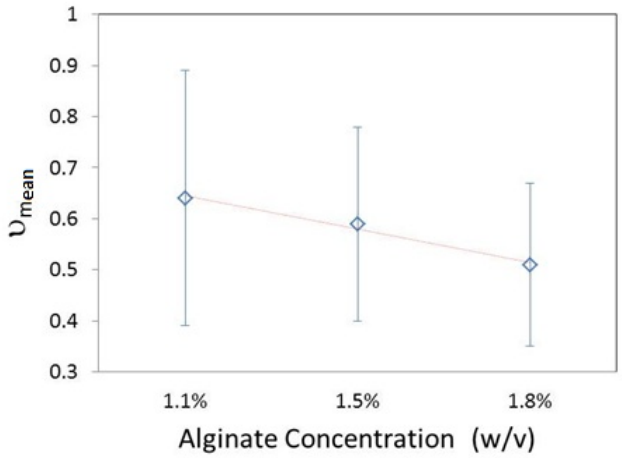

Figure 6: Relationship between average Poisson ratio and capsule composition.

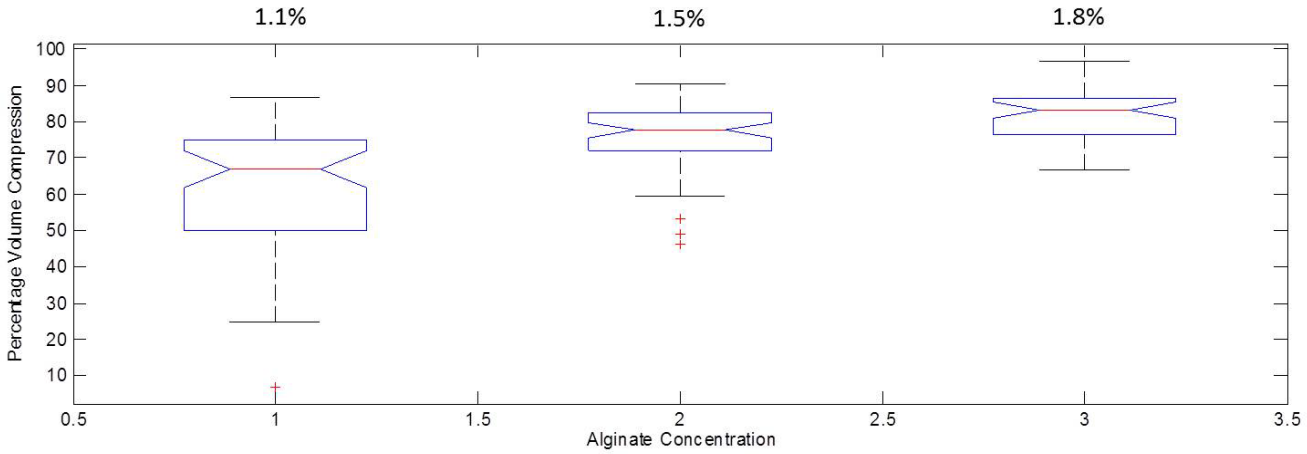

Figure 7: Box plot of percent volume compression as a function of capsule composition.

concentration. By analogy to the effect of capsule size on volume compression, it could safely be assumed that for the same cross-linker concentration, the higher the alginate concentration, the higher the number of cross-linked pores through which solvent loss occurred.

Discussion

Evidence of Poroelasticity

In light of the volume loss correlated to the number of cross-links as a function of capsule size (contact area) and alginate concentration, and, noisy strain measurements a strong case for the dominance of poroelasticity over viscoelasticity can be made [34-36]. The reported viscoelastic relaxation time (τ_v) is a few seconds for cross-linked hydrogels [39,40]. Using the approach to classify the time-dependent processes [11], which should occur under either the condition $t \sim \tau_v$ for viscoelastic relaxation or the condition $t \sim L^2/D$ for poroelastic relaxation, where t is the average recorded observation time of 120s and L is the radius of contact (~200 μm), the interpretation hinges upon the order of magnitude of the solvent diffusivity. The reported small molecule effective diffusivity (D_e) in 1.5% (w/v) alginate capsules averaging a few hundred microns is in the order of 10^{-12} m^2/s [49] and diffusivity D is in the order of $6.6*10^{-9}$ m^2/s for a cross-linked alginate slab [35]. When D_e was used then findings fell in the category of $t>>\tau_v$ and $t<<L^2/D$ =4000s inferring that viscoelastic relaxation has completed, but poroelastic relaxation has yet started, and the gel behaved like an elastic solid with relaxed moduli and with negligible migration of the solvent. When D was used then findings fell in the category of $t>>\tau_v$ and $t>>L^2/D$ =6s, both processes are relaxed, and the gel behaved like an elastic solid with relaxed moduli and with pronounced migration of the solvent. Results of compressive tests conducted on animal cells place the time of poroelastic relaxation over a length of micrometers to 10^{-1}s, and the time of poroelastic relaxation over a length of hundreds of micrometersis10^3s using an effective diffusivity of 10^{-11} m^2/s [40,41], the latter finding being closer to the experimental observation time of 120s.

Concentration Polarization

A marked study between the present work and other strain measurement efforts is the entrapment of blue dextran in the capsules. To this effect precautions were taken to avoid the convolution of the following interactions with strain measurements: 1) the capsules had reached an equilibrium swollen state post-fabrication monitored by microscopy, 2) the MW marker (blue dextran, MW=2×10^6 Da) chosen for the study did not react with the pores, 3) electrostatic and hydrophobic interactions at membrane interface were absent.

Multiple sources place the 70 kDa marker at the MW cutoff of the membrane [50]. In addition, the Stokes radius of this molecule estimated to be 9.2 nm is approximately double the pore size of the membrane measured by atomic force microscopy to be 4.5 nm ± 1.1 nm, 5.2 ± 0.9 nm and 5.7 ± 0.3 nm. Hence, diffusion was hindered for blue dextran and volume loss occurred by way of solvent efflux due to compression. It could also be assumed that the blue dextran was present in excess at the inner membrane interface to generate concentration polarization and thus block the pores. The higher the number of pores (alginate concentration), the higher was the resistance to deformation due to blocked pores contributing to increase stiffness at higher concentrations.

Conclusion

In this study, strain deformation results of hydrated alginate-based ASMs as a function of size and composition, confined in a microfluidic device were presented. Poroelastic deformation was observed independent of capsule size, with a statistically significant higher average ($p=1.4\times10^{-1}$, 95% CI) percent volume compression along with the tightest distribution occurring at an alginate concentration of 1.8% (w/v), characterized by an ideal mean Poisson ratio of 0.5. Other statistically significant findings were the smaller the ASMs, the lower the magnitude of average Poisson ratio and percent volume compression. For future clinical applications, the choice of the size/composition to use will depend on the specific drug to be encapsulated and the therapeutic window desired, requiring in turn for the ultrasound process parameters to be adjusted accordingly. Based on the findings of this study, for slow release the use of 500 μm and above capsules comprised of 1.1 % (w/v) alginate capsules are recommended. For fast release, the use of the 500 μm and smaller capsules comprised of 1.8% (w/v) alginate should be considered.

In order to reduce measurement uncertainty for strain deformation the following studies are recommended: 1) Use of 3D microscopy and or capsule deformation in the direction of compression, 2) Diffusivity measurements with MW markers matching the membrane pore size and 3) Strain measurements at multiple compression heights.

Acknowledgement

The authors would like to acknowledge the Davidson's College of Engineering Junior Faculty Development grants for funding this effort.

Declaration of interest

Authors have no declaration of interests to support.

References

1. Chang TMS (2013) Selected Topics in Nanomedicine. World Scientific Publishing.
2. Tamayol A, Akbari M, Annabi N, Paul A, Khademhosseini A, et al. (2013) Fiber-based tissue engineering: Progress, challenges, and opportunities. Biotechnol Adv 31: 669-687.
3. Mobed-Miremadi M, Nagendra RK, Ramachundrani SL, Rook JJ, Sridhar-Keralapura M, et al. (2013) Polystyrene microsphere and 5-Fluorouracil release from custom designed wound dressing film. Progress in Biomaterials 2 : 1-12.
4. Moura LI, Dias AM, Carvalho E, de Sousa HC (2013) Recent advances on the development of wound dressings for diabetic foot ulcer treatment--a review. Acta Biomater 9: 7093-7114.
5. Candiello J, Singh SS, Task K, Kumta PN, Banerjee I (2013) Early differentiation patterning of mouse embryonic stem cells in response to variations in alginate substrate stiffness. J Biol Eng 7: 9.
6. Capone SH, Dufresne M, Rechel M, Fleury MJ, Salsac AV, et al. (2013) Impact of alginate composition: from bead mechanical properties to encapsulated HepG2/C3A cell activities for in vivo implantation. PLoS One 8: e62032.
7. Ahearne M, Yang Y, El Haj AJ, Then KY, Liu KK (2005) Characterizing the viscoelastic properties of thin hydrogel-based constructs for tissue engineering applications. J R Soc Interface 2: 455-463.
8. Ferrara K, Pollard R, Borden M (2007) Ultrasound microbubble contrast agents: fundamentals and application to gene and drug delivery. Annu Rev Biomed Eng 9: 415-447.
9. Sridhar-Keralapura M, Thirumalai S, Mobed-Miremadi M (2013) Structural changes and imaging signatures of acoustically sensitive microcapsules under ultrasound. Ultrasonics 53: 1044-1057.
10. Agarwal A, FarouzY , Nesmith AP, DeraviLF, McCain ML et al. (2013) Micropatterning alginate substrates for in vitro cardiovascular muscle on a chip. Adv Funct Mater 23: 3738–3746.
11. Grassi M, Sandolo C, Perin D, Coviello T, Lapasin R, et al. (2009) Structural characterization of calcium alginate matrices by means of mechanical and release tests. Molecules 14: 3003-3017.

12. Anseth KS, Bowman CN, Brannon-Peppas L (1996) Mechanical properties of hydrogels and their experimental determination. Biomaterials 17: 1647-1657.
13. Storz H, Zimmermann U, Zimmerman H, Kuliche WM (2010) Viscoelastic properties of ultra-high viscosity alginates. Rheol Acta 49:155-167.
14. Hu Y, Suo Z (2012) Viscoelasticity and Poroelasticity in elastomeric gels. Acta Mechanica Solida Sinica 25: 441-458.
15. Yang CH, Wang MX, Haider H, Yang JH, Sun JY, et al. (2013) Strengthening alginate/polyacrylamide hydrogels using various multivalent cations. ACS Appl Mater Interfaces 5: 10418-10422.
16. Wang CX, Wang L, Thomas CR (2004) Modelling the mechanical properties of single suspension-cultured tomato cells. Ann Bot 93: 443-453.
17. Moura MJ, Figueiredo MM, Gil MH (2007) Rheological study of genipin cross-linked chitosan hydrogels. Biomacromolecules 8: 3823-3829.
18. Grigorescu G, Kulicke WM (2000) Prediction of Viscoelastic Properties and Shear Stability of Polymers in Solution. Adv Polym Sci 152: 1-40.
19. Zhao L, Zhang Z (2004) Mechanical characterization of biocompatible microspheres and microcapsules by direct compression. Artif Cells Blood Substit Immobil Biotechnol 32: 25-40.
20. Darling EM, Zauscher S, Block JA, Guilak F (2007) A thin-layer model for viscoelastic, stress-relaxation testing of cells using atomic force microscopy: do cell properties reflect metastatic potential? Biophys J 92: 1784-1791.
21. Forgacs G, Foty RA, ShafriY, Steinberg MS (1998) Viscoelastic properties of living embryonic tissues: a quantitative study. Biophysi J 74: 2227-2234.
22. Liu KK, Williams DR, Briscoe BJ (1996) Compressive deformation of a single microcapsule. Phys Rev E Stat Phys Plasmas Fluids Relat Interdiscip Topics 54: 6673-6680.
23. Gaumann A, Laudes M, Jacob B, Pommersheim R, Laue C, et al. (2000) Effect of media composition on long-term in vitro stability of barium alginate and polyacrylic acid multilayer microcapsules. Biomaterials 21: 1911-1917.
24. Sun G, Zhang Z (2001) Mechanical properties of melamine-formaldehyde microcapsules. J Microencapsul 18: 593-602.
25. Carin M, Barthès-Biesel D, Edwards-Lévy F, Postel C, Andrei DC (2003) Compression of biocompatible liquid-filled HSA-alginate capsules: determination of the membrane mechanical properties. Biotechnol Bioeng 82: 207-212.
26. Zhang Z, Saunders R, Thomas CR (1999) Mechanical strength of single microcapsules determined by a novel micromanipulation technique. J Microencapsul 16: 117-124.
27. Rachik M, Barthes-Biesel D, Carin M, Edwards-Levy F (2006) Identification of the elastic properties of an artificial capsule membrane with the compression test: effect of thickness. J Colloid Interface Sci 301: 217-226.
28. Salsac AV, Zhang L, Gherbezza JM (2009) Measurement of mechanical properties of alginate beads usingUltrasound, 19 ème Congrès Français de Mécanique.
29. Edwards-Lévy F, Lévy MC (1999) Serum albumin-alginate coated beads: mechanical properties and stability. Biomaterials 20: 2069-2084.
30. Ouwerx C, Velings N, Mestdagh M, Axelos M (1998) Physico-chemical properties and rheology of alginate gel beads formed with various divalent cations. Polym Gels Netw 6: 393-408.
31. Bartkowiak A, Hunkeler D (1999) Alginate-oligochitosan microcapsules: A mechanistic study relating membrane and capsule properties to reaction conditions. Chem Mat 11: 2486-2492.
32. Bartkowiak A, Hunkeler D (2000) Alginate-Oligochitosan Microcapsules II Control of mechanical resistance and permeability of the membrane. Chem Mat 12:206-212.
33. Kim K, Cheng J, Liu Q, Wu XY, Sun Y (2010) Investigation of mechanical properties of soft hydrogel microcapsules in relation to protein delivery using a MEMS force sensor. J Biomed Mater Res A 92: 103-113.
34. Hu Y, Zhao X, Vlassak JJ, Suo Z (2010) Using indentation to characterize the poroelasticity of gels. Appl Phys Lett 96: 121904.
35. Cai S, Hu Y, Zhao X, Suo Z (2010) Poroelasticity of a covalently crosslinked alginate hydrogel under compression JAP 108: 113514.
36. Hu Y, Chen X, Whitesides GM, Vlassak JJ, Suo Z (2001) Indentation of polydimethyl siloxane submerged in organic solvents 26: 785-795.
37. Constantinides G, Kalcioglu ZI, McFarland M, Smith JF, Van Vliet KJ (2008) Probing mechanical properties of fully hydrated gels and biological tissues. J Biomech 41: 3285-3289.
38. Kaufman JD, Miller GJ, Morgan EF, Klapperich CM (2008) Time-dependent mechanical characterization of poly(2-hydroxyethyl methacrylate) hydrogels using nanoindentation and unconfined compression. J Mater Res 23: 1472-1481.
39. Zhao X, Huebsch N, Mooney DJ, Suo Z (2010) Stress-relaxation behavior in gels with ionic and covalent crosslinks. J Appl Phys 107: 63509.
40. Charras GT, Mitchison TJ, Mahadevan L (2009) Animal cell hydraulics. J Cell Sci 122: 3233-3241.
41. Rosenbluth MJ, Crow A, Shaevitz JW, Fletcher DA (2008) Slow stress propagation in adherent cells. Biophys J 95: 6052-6059.
42. Duffy DC, McDonald JC, Schueller OJ, Whitesides GM (1998) Rapid Prototyping of Microfluidic Systems in Poly(dimethylsiloxane). Anal Chem 70: 4974-4984.
43. Prakash S, Chang TMS (1995) Preparation and in vitro analysis of microencapsulated genetically engineered E. coli DH5 cells for urea and ammonia removal. Biotechnol Bioeng 46: 621-626.
44. Choi AP, Zheng YP (2005) Estimation of Young's modulus and Poisson's ratio of soft tissue from indentation using two different-sized indentors: finite element analysis of the finite deformation effect. Med Biol Eng Comput 43: 258-264.
45. King M, Mody N (2011) Numerical and Statistical Methods for Bioengineering. Cambridge University Press, New York.
46. LeRoux MA, Guilak F, Setton LA (1999) Compressive and shear properties of alginate gel: effects of sodium ions and alginate concentration. J Biomed Mater Res 47: 46-53.
47. Chan ES, Lim TK, Voo WP, Pogaku R, Beng Ti Tey, et al. (2011) Effect of formulation of alginate beads on their mechanical behavior and stiffness. Particuology 9: 228-234.
48. Wan LQ, Jiang J, Arnold DE, Guo XE, Lu HH, et al. (2008) Calcium Concentration Effects on the Mechanical and Biochemical Properties of Chondrocyte-Alginate Constructs. Cell Mol Bioeng 1: 93-102.
49. Simpliciano C, Clark L, Asi B, Chu N, Mercado N, et al. (2013) Cross-Linked Alginate Film Pore Size Determination Using Atomic Force Microscopy and Validation Using Diffusivity Determinations, JSEMAT. 3: 1-12.
50. Mobed-Miremadi M, Asi B, Parasseril J, Tat M, Wong E, et al. (2013) Comparative Diffusivity Measurements for Alginate-Based Atomized and Inkjet-Bioprinted Artificial Cells using Fluorescence Microscopy. Art Cells Nanomed Biotechnol 41: 196 - 201.